

## Regional Variations in Shear Strength and Density of the Human Thoracic Vertebral Endplate and Trabecular Bone

Fred Xavier, Julio J. Jauregui, Nathan Cornish, Rebecca Jason-Rousseau, Dipal Chatterjee, Gavriel Feuer, Westley Hayes, Bhavleen H. Kapadia, John N. Carter, Hiroyuki Yoshihara and Subrata Saha

*Int J Spine Surg* 2017, 11 (1)

doi: <https://doi.org/10.14444/4007>

<https://www.ijssurgery.com/content/11/1/7>

This information is current as of April 30, 2025.

---

**Email Alerts** Receive free email-alerts when new articles cite this article. Sign up at:  
<http://ijssurgery.com/alerts>

# Regional Variations in Shear Strength and Density of the Human Thoracic Vertebral Endplate and Trabecular Bone

Fred Xavier, MD, PhD, Julio J. Jauregui, MD, Nathan Cornish, DO, Rebecca Jason-Rousseau, BS, Dipal Chatterjee, MD, Gavriel Feuer, PhD, Westley Hayes, MS, Bhavleen H. Kapadia, MD, John N. Carter, PhD, Hiroyuki Yoshihara, MD, PhD, Subrata Saha, PhD  
SUNY Downstate Medical Center, Brooklyn, New York, New York 11203

## Abstract

### Background

Previous studies investigated the overall mechanical strength of the vertebral body; however, limited information is available on the biomechanical properties of different regions within the vertebral endplate and cancellous bone. In addition, the correlation between mechanical strength and various density measurements has not been studied yet.

### Methods

Thoracic (T10) vertebrae were harvested from fifteen human cadaveric spines (average age: 77 years old). Twelve cylindrical cores of 7.2 mm (diameter) by 3.2 mm (height) were prepared from each vertebral body. Shear was produced using a stainless steel tubular blade and measured with a load cell from a mechanical testing machine. Optical and bulk densities were calculated before mechanical testing. Apparent, material, and ash densities were measured after testing.

### Results

Material density and shear strength increased from anterior to lateral regions of both endplate and cancellous bone. Endplate shear strength was significantly lower in the anterior ( $0.52 \pm 0.08$  MPa) than in the lateral region ( $2.72 \pm 0.59$  MPa) ( $p=0.017$ ). Trabecular bone maximum load carrying capacity was 5 times higher in the lateral ( $12 \pm 2.74$  N) ( $p=0.09$ ) and 4.5 times higher in the central ( $10 \pm 2.24$  N) ( $p=0.2$ ) than in the anterior ( $2 \pm 0.60$  N) regions. Mechanical strength positively correlated with ash density, and even more so with material density.

### Conclusion

Shear strength was the lowest at the anterior region and highest at the lateral region for both endplate and cancellous bone. Material density had the best correlation with mechanical strength. Newer spinal implants could optimize the loading in the lateral aspects of both endplate and cancellous bone to reduce the likelihood of screw loosening and the subsidence of disc replacement devices.

This study was reviewed by the SUNY Downstate Medical Center IRB Committee; IRB#: 533603-2.

BIOMECHANICS

KEYWORDS: VERTEBRAL FRACTURE, OSTEOPOROSIS, CANCELLOUS BONE, ENDPLATE, SHEAR STRENGTH, BONE DENSITY

VOLUME 10 ISSUE 1 DOI: 10.14444/4007

PAGES 41 - 49

## Introduction

When performing any surgical procedure within the spine, multiple factors should be considered.

Amongst these, lower bone quality may diminish the ability to achieve proper bone fixation, increase the loosening rates, cause hardware migration, and lead to a higher number of vertebral screws loosening, which would result in catastrophic surgical failures.<sup>1</sup>

Variations in the mechanical strength may also be ob-

served in non-surgical cases; for example, osteoporotic patients suffering from specific vertebral compression fractures may have different fracture patterns as a function of specific weaker areas within a vertebra. Although many studies have assessed the mechanical strength of the vertebral body, the specific biomechanical properties within different parts of the same vertebrae have not been widely studied. As such, the mechanical strength of different regions of endplate and cancellous bone are not fully under-

Downloaded from <https://www.ijssurgery.com/> by guest on April 30, 2025

stood.

Multiple methods have been employed to evaluate the density and strength within a vertebra. Some have evaluated the mechanical integrity through direct axial compression; either of the whole vertebral body or through selected segments of cancellous bone.<sup>2-4</sup> Halawa et al. (1978) studied the shear strength of the femoral epiphyseal cancellous bone to assess the mechanisms of interlocking of polymethylmethacrylate (PMMA) with the adjacent bone after joint replacement surgeries. Shear strength of the trabecular bone was considered to be more important than its compressive strength considering that implant loosening usually happens through a failure in shear at the bone-implant interface.<sup>5</sup> A similar failure mechanism could be expected with various implants used in spinal fusion and disc replacement surgeries. Strong vertebral screw purchase is critical to maintain stability, avoid micromotion, and prevent loosening. Dual energy x-ray absorptiometry (DEXA) scanning is widely used to measure the overall density of bone. Several studies have described that the outcomes of the scan are strongly correlated to the overall mechanical strength. Although DEXA scans have many advantages, this image modality may not accurately define the density within specific regions of a vertebral bone.

The correlation between the mechanical strength of vertebral cancellous bone and various density measurements is not entirely understood. Evaluating the bone volume fraction is critical to the understanding of porosity and to assess the mechanical properties of trabecular bone. This can be understood as a fraction, which is a ratio of the bone material volume (BV) over tissue or total volume (TV), and can depict how two different cancellous structures could have the same bone fraction (BV/TV) depending on the apparent and the material density values. Apparent density ( $D_{app}$ ) correlates with the bone tissue mechanics, whereas material density ( $D_{mat}$ ) influences the bone properties at the trabecular level.<sup>6</sup> As described by Zioupos et al.,  $D_{app}$  and the  $D_{mat}$  are negatively correlated. They showed that increases in the apparent density were accompanied with an associated decrease in the material density of the trabeculae.<sup>6</sup>

Although, previous studies have analyzed the mechanical strength of the endplate, using compressive force,<sup>7</sup> a detailed analysis of cancellous bone structure at the various anatomical regions has not been performed yet. To the best of our knowledge, no other published studies have investigated the regional changes in density and shear strength within the vertebral cancellous bone. Therefore, the purpose of this study was to evaluate the biomechanical properties of vertebral trabecular bone and endplate. More specifically, we analyzed and compared the differences between the anterior, central, and lateral part of the human thoracic vertebral body. We then assessed the correlations between porosity, density, and shear strength for both trabecular bone and endplate.

## Materials & Methods

### Specimen Preparation

The tenth thoracic vertebrae (T10) from fifteen embalmed human cadaveric spines were harvested and stored at -20°C. There were 9 male and 6 female cadavers with a mean age of 77 years (range, 47 to 98 years). Subsequently, we used a trephine to obtain twelve cylindrical cores measuring 7.24 mm (diameter) by 3.15 mm (height); six vertebral endplate samples (with subchondral bone) and six cancellous bone samples. The bony endplates were labeled as cranial (superior) or caudal (inferior) relative to the vertebra (not the disc) (Figure 1 and Figure 2).

### Mechanical Testing

The specimens were tested using a mechanical testing machine (Instron 5566, Instron, Norwood, Massachusetts, USA). As described by Mitton et al.,<sup>8</sup> a sharpened stainless steel tube, which cuts through the bone during axial loading, was used to apply shear force (Figure 3). Load was applied at a deformation rate of 1 mm/min (Instron 5566 – 10 kN load cell), leading to the characteristic load-deformation curves (Figure 4). In an attempt to recreate a more physiological environment during testing, all samples were maintained hydrated with a physiological saline bath (0.9% non-buffered NaCl) at  $37^{\circ} \pm 1^{\circ}\text{C}$  (Figure 3). We utilized and implemented two previously developed and validated methods of shear testing.<sup>8</sup>

Method (1): The global method gave a shear strength based on the maximum shear obtained during the loading experiment:

$$\tau_{max} = \frac{1}{2\pi r} \times \frac{F_{max}}{LF_{max}}$$

Where:

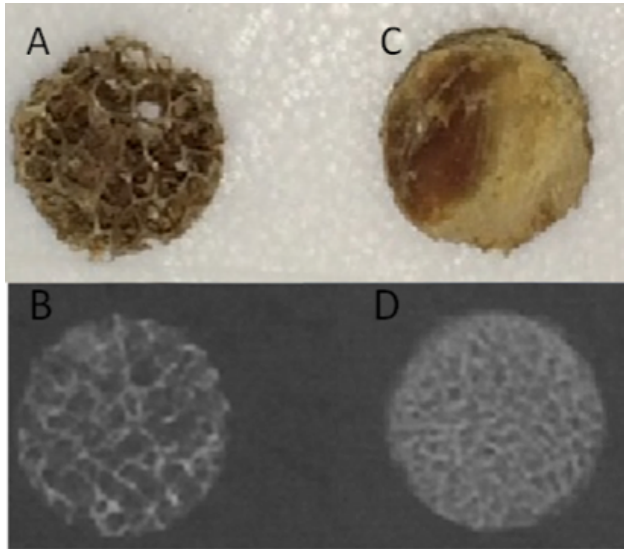


Fig. 1. Cored cylindrical vertebral specimens before testing. Cancellous bone (A); Endplate with subchondral bone (C). Faxitron X-ray of cancellous bone (B) and endplate with subchondral bone (D). Diameter: 7.24 mm; Height: 3.15 mm. Note the difference in porosity between endplate and cancellous bone.

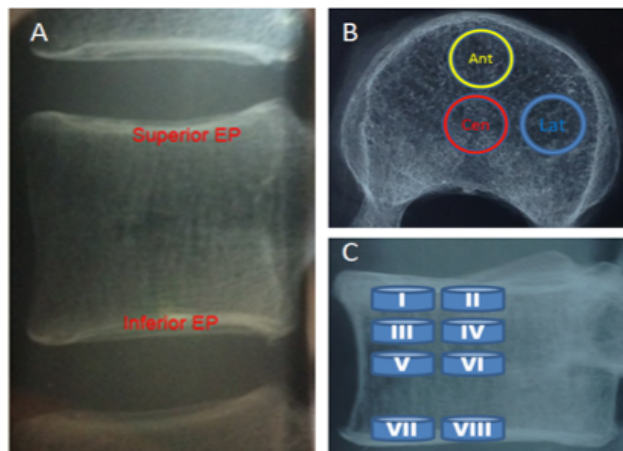


Fig. 2. Plain radiographs of thoracic vertebrae. A) Lateral view of a segment of the thoracic column. B) Axial view of a thoracic vertebra showing the different regions: anterior, central, and lateral. C) Lateral view: I- Endplate anterior superior (EP Ant Sup); II- Endplate central superior (EP Cen Sup); III- Cancellous anterior superior (Ant Sup); IV- Cancellous central superior (Cen Sup); V- Cancellous anterior middle (Ant Mid); VI- Cancellous central middle (Cen Mid); VII- Endplate anterior inferior (EP Ant Inf); VIII- Endplate central inferior (EP Cen Inf).

$\tau_{max}$  (MPa) = maximum or global shear strength;

$F_{max}$  (N) = maximum load to failure;

$LF_{max}$  (mm) = displacement at maximum load to failure;

$r$  (mm) = inner diameter of the stainless steel tube.

Method (2): The incremental method produced the mean elementary shear strength that depended on the average positive slope of smaller sections of the curve:

$$\tau_{elm} = \frac{1}{2\pi r} \times MPS$$

Where:

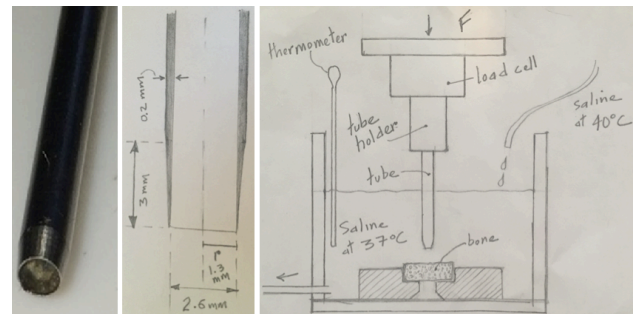


Fig. 3. Stainless tube used for shear testing (left). Diagram showing the tube ending details (center). Diagram showing the apparatus for shear testing with the regulated saline bath at 37°C (right).

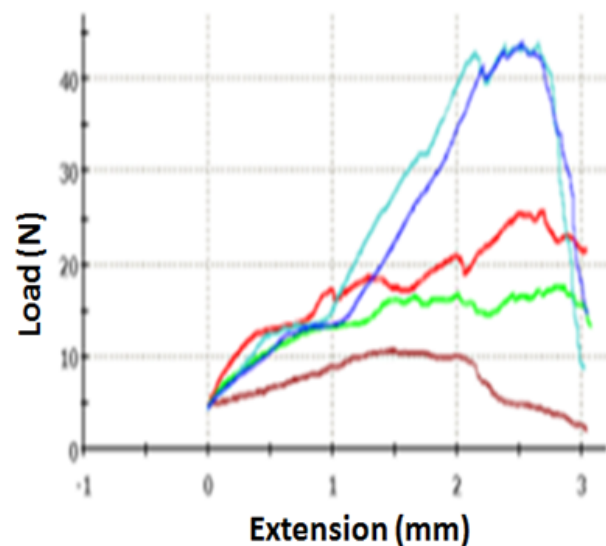


Fig. 4. Load-displacement curves from shear testing of five specimens.

$\tau_{\text{elem}}$  (MPa) = mean elementary shear strength;

MPS = mean of the slope.

### Density Measurements

Optical and bulk densities were calculated before mechanical testing whereas apparent, material, and ash densities were measured after the testing. Optical areal density ( $D_{\text{opt}}$ ) measurements were performed using identical cored bone discs radiographed alongside an aluminum wedge using a Faxitron X-ray<sup>TM</sup> (Faxitron Bioptics, LLC, Tucson, Arizona, USA) machine. After scanning the radiographs at 400 DPI, grayscale images were obtained and uploaded into ImageJ.<sup>9</sup> The mean pixel value of a region of interest representing the entire area of each sample was calculated. Conversion from pixel intensity to areal density ( $\text{g}/\text{cm}^2$ ) was calculated based on the known density along the aluminum wedge.

The bulk (or wet) density ( $D_{\text{bulk}}$ ) was calculated as the ratio of the wet specimen (bone tissue with marrow) weight (g) over the gross sample volume ( $\text{cm}^3$ ). We measured the dimensions with a digital caliper (Mitutoyo<sup>TM</sup>, Kawasaki, Japan) to the nearest 0.01 mm.

$$D_{\text{bulk}} = \frac{W_{\text{wet}}}{V_0}$$

After mechanical testing, apparent density ( $D_{\text{app}}$ ) of each sample was derived from the ratio of dry weight over gross volume. Samples were dried after being chemically de-fatted (ethanol 100% for 24 hours, air dried, and left at room temperature for 48 hours).

$$D_{\text{app}} = \frac{W_{\text{dry}}}{V_0}$$

Material density of the trabecular bone material ( $D_{\text{mat}}$ ) was measured with an electronic microbalance (Mettler Toledo<sup>®</sup> College B154, Mettler Toledo, Greifensee, Switzerland) based on the Archimedes' principle. The specimens were immersed in 100% ethanol (specific density  $\sim 0.7 \text{ g}\cdot\text{cm}^{-3}$ ) and the weight was measured.

$$D_{\text{mat}} = \rho \times \frac{W_{\text{dry}}}{(W_{\text{dry}} - W_{\text{sub}})}$$

The ratio of bone volume / total volume (BV/TV) and porosity were also calculated.

$$\frac{BV}{TV} = \frac{D_{\text{app}}}{D_{\text{mat}}}$$

$$\text{Porosity} (|\%) = 100 \times \left[ 1 - \frac{BV}{TV} \right]$$

$W_{\text{wet}}$  (g): wet (bone tissue) weight;  $W_{\text{dry}}$  (g): dry weight;  $V_0$  ( $\text{cm}^3$ ): gross sample volume;  $W_{\text{sub}}$  (g): submerged weight.

Ash density was measured after performing the mechanical testing and the material density measurements. The samples were dried at room temperature for 48 hours, weighted, and heated in a furnace at  $700^\circ\text{C}$  for 6 hours. Ash content was calculated by dividing the ash weight by the dry weight of the sample. Then, ash density was obtained as the ratio of ash weight over the volume (derived from the Archimedes' Principle).

### Statistical Analysis

Global differences in mechanical shear strength and structural properties between the anatomical regions were investigated using SPSS Statistics software (version 17.0) and GraphPad Prism (version 6.00 for Windows, GraphPad Software, La Jolla California USA). To assess the statistical significant differences (accepted at  $p \leq 0.05$ ) in density and mechanical strength between anterior, central, and lateral regions, we used one-way analysis of variance (ANOVA) and Tukey post-hoc test. A Mann-Whitney test was used to evaluate the significant differences (accepted at  $p \leq 0.05$ ) between superior and inferior endplates. Linear regression and the Pearson's correlation coefficient ( $r^2$ ) were used to determine correlations among the variables.

## Results

The overall density profile varied within different regions of the vertebral cancellous bone (Figure 5).

When comparing the optical density, we found that



this density doubled from the lateral to the anterior and from the central to the anterior region, which was found to be statistically significant ( $p = 0.01$  and  $0.01$ ). We also found an increase in the bulk density of 22% from the lateral to the anterior region and of 27% from the central to the anterior region of the cancellous bone ( $p = 0.12$  and  $0.06$ ). However, trabecular material and ash densities were slightly lower at the anterior than in the lateral and central regions ( $p > 0.05$ ). We also found that specimens obtained from female cadavers had higher bulk and optical, but lower material and ash density values.

In terms of mechanical strength, we found that the anterior region of the cancellous bone was weaker than the lateral and central portions in both shear strength and maximum load to failure, although not statistically significant (Figure 6 and Table 1).

Density varied within the vertebral endplate, following a similar pattern to the cancellous bone. Endplate optical density was higher in the anterior than in the

lateral regions ( $p = 0.05$ ) (Figure 7). However, material density measurements showed that the anterior endplate was 9% less dense than the lateral ( $p = 0.023$ ) and 10% less dense than the central portions ( $p = 0.016$ ). When comparing the overall density of the superior endplates (SEPs) to the inferior endplates (IEPs), we found that bulk and material density were slightly lower in the SEPs, whereas the ash density was lower in the IEPs ( $p > 0.05$ ). Interestingly, we observed a 15% increase in endplate bulk density in female ( $p = 0.01$ ). However, the male specimens showed higher material and ash density values ( $p > 0.05$ ).

The anterior endplate was mechanically weaker than both the lateral and central regions (Figure 8 and Table 1). In regards to the shear strength, we found a significantly lower strength at the anterior portion of the endplate than at the lateral region ( $0.52 \pm 0.08$  MPa versus  $2.72 \pm 0.59$  MPa;  $p = 0.02$ ). The mean maximum load carrying capacity was six times higher in the lateral endplate compared to the anterior endplate ( $p = 0.01$ ). The central endplate region appeared stronger than the anterior part in both shear and maximum load carrying capacity ( $p = 0.19$  and  $0.19$ , respectively). From the inferior to the superior endplates, shear strength and maximum load to failure decreased by 23% and 33%, respectively ( $p > 0.05$ ).

As shown in Table 2, the mechanical strength positively correlated with apparent, trabecular material and ash densities. However, we observed a negative correlation between mechanical strength and both

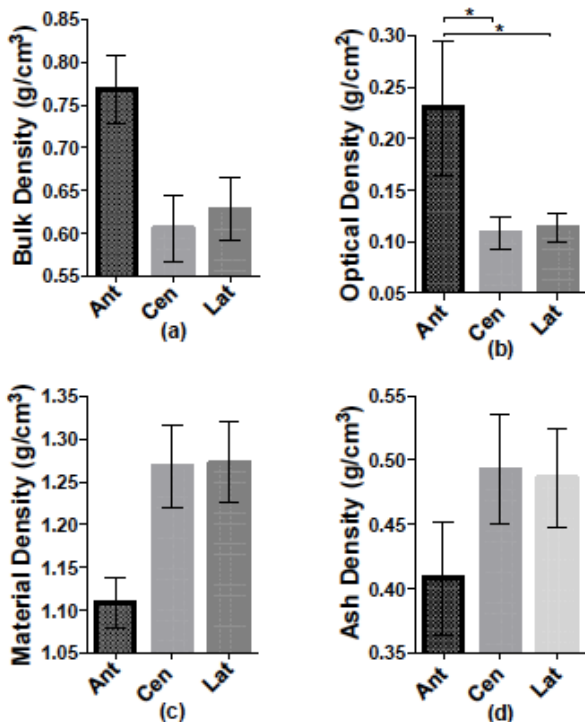


Fig. 5. Mean (SE) density values for the three main regions of the cancellous bone. a) bulk density (g/cm<sup>3</sup>); b) optical density (g/cm<sup>2</sup>); c) material density (g/cm<sup>3</sup>); d) ash density (g/cm<sup>3</sup>). \*:  $p < 0.05$ . Anterior (N = 10); Central (N = 26); Lateral (N = 27). Note that the anterior (ant) region had higher bulk and optical density values than the central (cen) and lateral (lat) regions. However, the anterior region had the lowest material and ash density values.

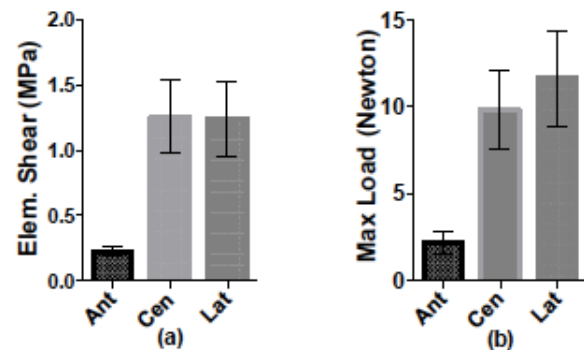


Fig. 6. Figure 6. Mean (SE) cancellous bone elemental shear strength and maximum load to failure. Anterior (N = 10); Central (N = 26); Lateral (N = 27).

optical and bulk densities. Material and ash density values also correlated negatively with the level of spinal osteoarthritis based on the Kelgreen-Lawrence scale (Table 3). However, we found that both bulk and optical density values increased with the degree of osteoarthritis.

## Discussion

The purpose of this study was to assess the variations in density and mechanical strength across the

**Table 1. Regional changes in vertebral mechanical properties.**

		Endplate			Cancellous		
		Lateral	Central	% Decrease	Lateral	Central	% Decrease
Elem Shear	M	3.09 (0.71)	2.11 (0.53)	32	1.50 (0.37)	1.56 (0.39)	-4
	F	1.98 (1.09)	1.49 (0.75)	25	0.80 (0.42)	0.68 (0.29)	14
Glob Shear	M	1.91 (0.51)	1.74 (0.48)	9	0.87 (0.26)	0.72 (0.22)	18
	F	1.62 (0.89)	1.14 (0.55)	30	0.46 (0.24)	0.34 (0.14)	25
Max Load	M	41.29 (10.43)	28.22 (6.79)	32	13.87 (3.49)	11.98 (3.03)	14
	F	24.28 (13.27)	15.45 (6.93)	36	7.88 (4.37)	5.86 (2.83)	26
		Endplate			Cancellous		
		Lateral	Anterior	% Decrease	Lateral	Anterior	% Decrease
Elem Shear	M	3.09 (0.71)	0.44 (0.06)	86 *	1.50 (0.37)	0.25 (0.08)	83
	F	1.98 (1.09)	0.60 (0.14)	70	0.80 (0.42)	0.20 (0.02)	75
Glob Shear	M	1.91 (0.51)	0.37 (0.07)	81	0.87 (0.26)	0.19 (0.08)	78
	F	1.62 (0.89)	0.55 (0.07)	66	0.46 (0.24)	0.16 (0.06)	64
Max Load	M	41.29 (10.43)	5.14 (1.03)	88 *	13.87 (3.49)	3.02 (1.07)	78
	F	24.28 (13.27)	6.47 (2.02)	73	7.88 (4.37)	1.33 (0.39)	83

Units of shear (elemental and global) strength and maximum load to failure are in MPa and N, respectively. Values represent the mean (SEM) of cancellous (median and superior combined) and endplate (inferior and superior combined). Changes are given as percentage of decrease from lateral to central and from lateral to anterior. Statistical significance (\*:  $p < 0.05$ ). M: male; F: female. Note the reduction in mechanical strength of 9% to 36% from lateral to central and of 66% to 88% from lateral to anterior (both endplates and cancellous bone).

different regions of the thoracic vertebral body. To the best of our knowledge, we are the first to investigate the regional changes within the vertebral cancellous bone. Material and ash densities were the lowest

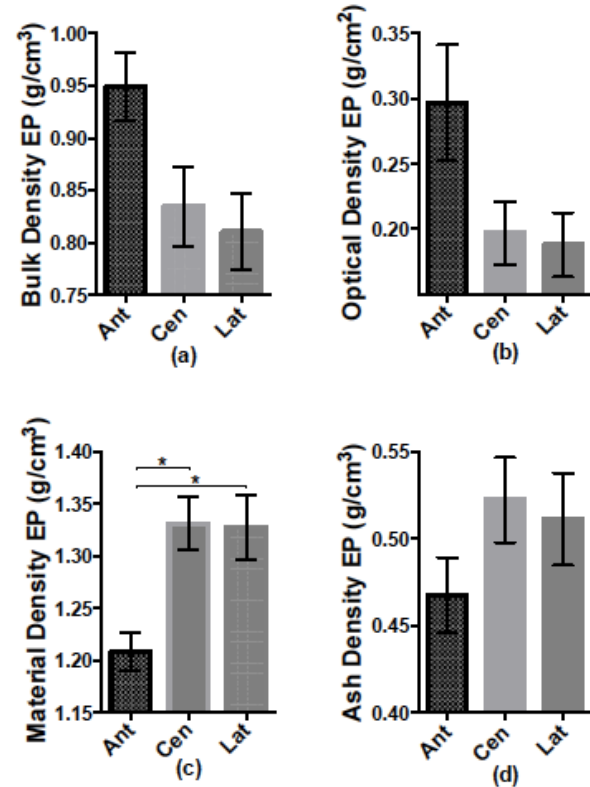


**Fig. 7.** Mean (SE) density values for the three main regions of the vertebral endplate (EP). a) bulk density (g/cm<sup>3</sup>); b) optical density (g/cm<sup>2</sup>); c) material density (g/cm<sup>3</sup>); d) ash density (g/cm<sup>3</sup>). \*:  $p < 0.05$ . Anterior (N = 14); Central (N = 28); Lateral (N = 24). Note that the anterior (ant) region had higher bulk and optical density values than the central (cen) and lateral (lat) regions. However, the anterior region had the lowest material and ash density values.

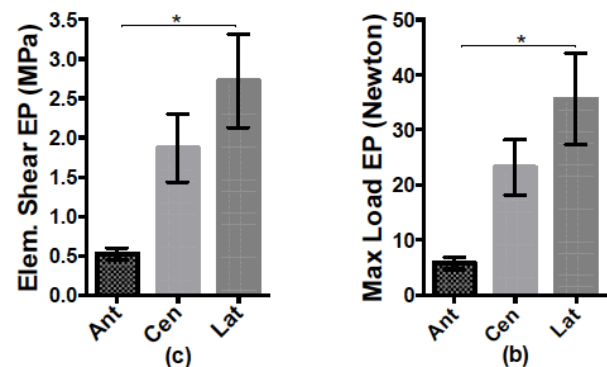


**Fig. 8.** Mean (SE) vertebral endplate (EP) elemental shear strength and maximum load to failure. Anterior (N = 14); Central (N = 28); Lateral (N = 24). \*:  $p < 0.05$ . The anterior region was significantly weaker than the lateral region for elemental shear strength ( $p = 0.017$ ) and maximum load to failure ( $p = 0.012$ ).

in the anterior parts of the cancellous bone, although not significant. Similarly, material density measurements showed that the anterior endplate was significantly less dense than both lateral and central re-

**Table 2. Pearson correlation between mechanical strength, density, osteoarthritis level (K-L Score), and age.**

Vertebral Endplate								
		K-L Score	Age	Dbulk	Dapp	Dmat	Dopt	Dash
Elem Shear	M	-.364*	.108	-.364*	.440**	.440**	-.493**	.337*
	F	-.614**	-.677**	-.635**	.739**	.744**	-.362	.523**
Glob Shear	M	-.427**	.009	-.300	.507**	.507**	-.395*	.393*
	F	-.602**	-.682**	-.605**	.713**	.719**	-.330	.506**
Max Load	M	-.489**	-.019	-.260	.419**	.419**	-.381*	.321*
	F	-.602**	-.670**	-.592**	.717**	.721**	-.356	.524**
Vertebral Cancellous Bone								
		K-L Score	Age	Dbulk	Dapp	Dmat	Dopt	Dash
Elem Shear	M	-.615**	-.193	-.059	.368*	.605**	-.316	.548**
	F	-.837**	-.679**	-.471*	.527**	.811**	-.546**	.840**
Glob Shear	M	-.367*	-.005	.003	.460**	.615**	-.154	.539**
	F	-.837**	-.678**	-.439*	.544**	.787**	-.465*	.819**
Max Load	M	-.571**	-.167	-.069	.437**	.574**	-.273	.495**
	F	-.825**	-.690**	-.464*	.560**	.815**	-.506*	.844**

Values represent  $r^2$ . Negative sign (-) is for a negative correlation whereas an absence of sign stands for a positive one. M: male; F: female; K-L Score: Kelgren-Lawrence score; Dbulk: bulk density; Dapp: apparent density; Dmat: material density; Dopt: optical density; Dash: ash density. \*\*:Correlation is significant at 0.01 at the level (2-tailed). \*:Correlation is significant at 0.05 at the level (2-tailed).

gions. Other studies explored this variation within the endplate using radiological measurements. Muller-Gerbl (2008) examined the regional distribution of mineralization across the cervical endplates using computed tomographic osteoabsorptiometry (CT-OAM). The posterolateral regions were significantly the most mineralized, whereas the anterior regions were the least dense.<sup>10</sup>

The overall mechanical properties of the cancellous bone decreased by an average of 15% from the lateral to the central regions and by 75% from the lateral to the anterior regions, although not significant ( $p>0.05$ ). However, there was a significant five-fold increase in strength from anterior to lateral regions of the endplate ( $p<0.05$ ). Our results are in accordance with those of Lowe et al. (2004) who investigated the resistance of the human vertebral endplate by applying compressive loads, utilizing hollow and solid indenters to different regions of the endplate. They found that the highest maximum load to failure values for thoracic vertebrae were in the posterolateral regions of the endplate as opposed to the center and anterior areas. Similarly, a study by Grant et al. (2001) mapped the mechanical strength of the human lumbosacral (L3-S1) vertebral endplates. After removal of the intervertebral discs, twenty-seven spots were tested with a 3-mm-diameter hemispherical indenter pressed into the endplate surface. They found that the posterior test sites were 3.1 times stronger than the anterior ones.<sup>7</sup> Although not statistically significant, we observed that the inferior endplates were denser and stronger than the superior ones. Previous studies have shown significant in-

**Table 3. Pearson correlation between density measurements, osteoarthritis level (K-L Score), and age.**

Vertebral Endplate							
		Age	Dbulk	Dapp	Dmat	Dopt	Dash
K-L Score	M	.627**	.367*	-.353*	-.353*	.338*	-.039
	F	.428*	.680**	-.510**	-.504**	.354	-.355
Age	M	1	.189	.073	.073	-.228	.290
	F	1	.342	-.525**	-.570**	-.136	-.273
Vertebral Cancellous Bone							
		Age	Dbulk	Dapp	Dmat	Dopt	Dash
K-L Score	M	.686**	.372*	-.364*	-.568**	.260	-.502**
	F	.628**	.463*	-.513*	-.746**	.323	-.763**
Age	M	1	.309	-.168	-.344*	-.277	-.311
	F	1	.186	-.399	-.843**	-.059	-.694**

Values represent  $r^2$ . Negative sign (-) is for a negative correlation whereas an absence of sign stands for a positive one. M: male; F: female; K-L Score: Kelgren-Lawrence score; Dbulk: bulk density; Dapp: apparent density; Dmat: material density; Dopt: optical density; Dash: ash density. \*\*: Correlation is significant at 0.01 at the level (2-tailed). \*: Correlation is significant at 0.05 at the level (2-tailed).

Downloaded from <https://www.ijssurgery.com/> by guest on April 30, 2025



crease in both load to failure and stiffness from the superior to the inferior endplates.<sup>7,10,11</sup> Lowe et al. (2004) found no statistically significant differences in mechanical strength between inferior and superior endplates obtained from thoracic and lumbar specimens.<sup>12</sup>

The values of shear stress from this work are in accord with those from previous biomechanical studies. Evans and King (1961) performed mechanical testing (via uniaxial stress) on femoral cancellous bone from an embalmed cadaver and reported that the strength of the specimens ranged from 0.21 to 14.82 MPa.<sup>13</sup> McElhaney et al. (1970) tested vertebral bodies, characterized as 'fresh frozen' and found that the specimen exhibited a strength of 4.13 MPa after being exposed to uniaxial stress.<sup>14</sup> Saha and Gorman (1981) and Stone et al. (1983) found an average cancellous shear strength which ranged between 5 – 7 MPa.<sup>15,16</sup>

Vertebral endplate and cancellous bone tissues obtained from the lateral regions had much greater material density, ash content, and mechanical strength than anterior samples. However, bulk and optical densities were significantly higher in the anterior regions. This could be due to the presence of greater amount of necrotic tissue in the anterior region of the vertebral body as mentioned in previous studies.<sup>17-19</sup> A similar density pattern was observed between male and female samples. Male specimens had greater mechanical strength, material and ash densities. This difference could be explained, in part, by the age difference between male and female cadavers (mean age of 72 versus 85 years). However, bulk and optical densities were significantly higher in female samples. Potentially, this could be due to a greater amount of soft tissue (i.e. bone marrow) in the pores of female cancellous samples, which may increase the 'gross' density without any gain in bone material content and mechanical strength. Note that optical and bulk densities were calculated on intact bone tissue, before the treatment with ethanol. Material and ash densities were determined after defatting to properly access the mass and volume of the trabeculae.

This study had several limitations. Due to our relatively small sample size, our findings may be under-

powered. This could be the reason why no statistical differences were found in the cancellous groups despite the obvious and sometimes wide gap in values, especially between the anterior and the lateral regions.

In addition, we utilized embalmed samples instead of fresh cadavers as suggested by several studies.<sup>20,21</sup> However, other studies like the one by Topp et al. (2012) have described similar stiffness and fracture patterns between both types of samples. Additionally, they described differences, which were not significant in screw pullout forces and axial maximum load to failure for cancellous and cortical screws.<sup>22</sup> Moreover, we evaluated differences between regions of the same embalmed samples, which diminish potential limitations caused by not utilizing fresh cadavers.

## Conclusion

We explored the variations in biomechanical properties within the thoracic vertebral cancellous bone and endplate. Density and shear strength were the lowest in the anterior region of the vertebral bodies for both endplate and cancellous bone. Newer implants for spinal interbody fusion could optimize the load distribution in the lateral aspects instead of the anterior aspects of the endplate. Although we did not find any differences between the central and the lateral regions of the lower thoracic (T10) cancellous bone, further studies could follow our path and use much larger sample size. This relationship might also be assessed at the upper thoracic, cervical and lumbar spinal segments. Such studies could provide meaningful data for pullout strength of the screws used in anterior spinal plating system.

## References

1. Cheng XG, Nicholson PH, Boonen S, et al. Prediction of vertebral strength in vitro by spinal bone densitometry and calcaneal ultrasound. *Journal of Bone and Mineral Research*. 1997;12(10):1721-1728.
2. Carter DR, Hayes WC. The compressive behavior of bone as a two-phase porous structure. *The Journal of Bone & Joint Surgery*. 1977;59(7):954-96
3. Goulet RW, Goldstein SA, Ciarelli MJ, Kuhn JL,

Brown M, Feldkamp L. The relationship between the structural and orthogonal compressive properties of trabecular bone. *Journal of biomechanics*. 1994;27(4):375-389.

4. Linde F. Elastic and viscoelastic properties of trabecular bone by a compression testing approach. *Danish Medical Bulletin*. 1994;41(2):119-13

5. Halawa M, Lee A, Ling R, Vangala S. The shear strength of trabecular bone from the femur, and some factors affecting the shear strength of the cement-bone interface. *Archives of orthopaedic and traumatic surgery*. 1978;92(1):19-30.

6. Zioupos P, Cook RB, Hutchinson JR. Some basic relationships between density values in cancellous and cortical bone. *Journal of biomechanics*. 2008;41(9):1961-1968.

7. Grant JP, Oxland TR, Dvorak MF. Mapping the structural properties of the lumbosacral vertebral endplates. *Spine*. 2001;26(8):889-896.

8. Mitton D, Rumelhart C, Hans D, Meunier P. The effects of density and test conditions on measured compression and shear strength of cancellous bone from the lumbar vertebrae of ewes. *Medical Engineering and Physics*. 1997;19(5):464-474.

9. Rasband W. WS 1997–2014. ImageJ. US National Institutes of Health, Bethesda, Md.

10. Muller-Gerbl M, Weisser S, Linsenmeier U. The distribution of mineral density in the cervical vertebral endplates. *Eur Spine J*. 2008;17(3):432-438.

11. Grant JP, Oxland TR, Dvorak MF, Fisher CG. The effects of bone density and disc degeneration on the structural property distributions in the lower lumbar vertebral endplates. *J Orthop Res*. 2002;20(5):1115-1120.

12. Lowe TG, Hashim S, Wilson LA, et al. A biomechanical study of regional endplate strength and cage morphology as it relates to structural interbody support. *Spine*. 2004;29(21):2389-2394.

13. Evans FG, King AI. Regional differences in some physical properties of human spongy bone. *Biomechanical studies of the musculo-skeletal system*. 1961:49-6

14. McElhaney JH, Fogle JL, Melvin JW, Haynes RR, Roberts VL, Alem NM. Mechanical properties of cranial bone. *Journal of Biomechanics*. 1970;3(5):495-511.

15. Saha S, Gorman P. Strength of human cancellous bone in shear and its relationship to bone mineral content. *Transactions of the 27th Annual Orthopaedic Research Society*. 1981;21

16. Stone JL, Beaupre GS, Hayes WC. Multiaxial strength characteristics of trabecular bone. *Journal of biomechanics*. 1983;16(9):743-752.

17. Chou LH, Knight RQ. Idiopathic avascular necrosis of a vertebral body. Case report and literature review. *Spine (Phila Pa 1976)*. 1997;22(16):1928-1932.

18. Kaneda K, Asano S, Hashimoto T, Satoh S, Fujiya M. The treatment of osteoporotic-posttraumatic vertebral collapse using the Kaneda device and a bioactive ceramic vertebral prosthesis. *Spine*. 1992;17:295-303.

19. Young WF, Brown D, Kendler A, Clements D. Delayed post-traumatic osteonecrosis of a vertebral body (Kummell's disease). *Acta Orthop Belg*. 2002;68(1):13-1

20. Hubbard RP. Flexure of layered cranial bone. *J Biomech*. 1971;4(4):251-263.

21. Currey JD, Brear K, Zioupos P, Reilly GC. Effect of formaldehyde fixation on some mechanical properties of bovine bone. *Biomaterials*. 1995;16(16):1267-1271.

22. Topp T, Müller T, Huss S, et al. Embalmed and fresh frozen human bones in orthopedic cadaveric studies: which bone is authentic and feasible? A mechanical study. *Acta orthopaedica*. 2012;83(5):543-547.

## Disclosures & COI

Bhaveen Kapadia is a consultant for and on the speakers bureau of Sage Products, LLC. The other authors declare no relevant disclosures or conflicts of interest.

## Corresponding Author

Fred Xavier, MD, PhD, SUNY Downstate Medical Center, 450 Clarkson Avenue - Box 30, Brooklyn, New York 11203. Fredxavier7@gmail.com.

Published 27 February 2017.

This manuscript is generously published free of charge by ISASS, the International Society for the Advancement of Spine Surgery. Copyright © 2017

ISASS. To see more or order reprints or permissions,  
see <http://ijssurgery.com>.